IL NUOVO CIMENTO Vol. 32 C, N. 5-6 Settembre-Dicembre 2009
DOI 10.1393/ncc/i2010-10530-4

Colloquia: LaThuile09

Search for high-mass Standard Model Higgs at the Tevatron

H. Greenlee for the CDF and D0 Collaborations
Fermi National Accelerator Laboratory - Batavia, IL, USA

(ricevuto il 10 Novembre 2009; pubblicato online il 18 Gennaio 2010)

Summary. — In this paper, we present results on searches for Standard Model Higgs boson production in the channels $H \to WW \to \ell^+\ell^-$, $WH \to WWW \to \ell^\pm\ell^\pm$, and $H \to \gamma\gamma$. No evidence for the Higgs boson is observed, and we set upper bounds on Higgs boson production. Taking into account Standard Model predictions for Higgs boson production and decay, the existence of the Standard Model Higgs boson is excluded at 95% CL for $m_H = 170\,\text{GeV}$.

PACS 14.80.Bn – Standard-model Higgs bosons.

The Standard Model of elementary-particle physics with three generations of quarks and leptons is very successful at explaining phenomena associated with strong, weak, and electromagnetic interactions. In addition to the observed fermions and gauge bosons, the consistency of the Standard Model requires the existence of a "Higgs sector" containing one or more scalar fields to regulate the ultraviolet behavior of the theory. In the simplest case, there is one Higgs doublet, which leads to a single physical scalar particle, which is the "Standard Model Higgs boson". The mass of the Higgs boson is not predicted by the theory. However, once the mass of the Higgs boson is specified, there are no other free parameters, and all interactions of the Higgs boson are determined.

Experimental constraints on the Higgs boson mass come from direct searches at LEP [1], which put a lower limit on the Higgs boson mass of 114.4 GeV, and from precision electroweak measurements that are sensitive to the effects of higher-order corrections involving virtual Higgs particles [2]. The latter predict a Higgs boson mass of $m_H = 84^{+34}_{-26}\,\text{GeV}$, or $m_H < 154\,\text{GeV}$ at 95% CL.

1. – Experiments and data samples

The results presented in this paper are based on data collected as part of Tevatron collider Run II, which began in April 2002 and is still continuing, in which protons and antiprotons collide at $\sqrt{s} = 1.96\,\text{TeV}$. Data from from both Tevatron experiments, CDF and D0, are included. The combined Higgs boson results shown here are from the "summer 2008" Tevatron Higgs combination [3], although some individual channels have been updated since then. A typical integrated luminosity for channels included in the

© Società Italiana di Fisica / INFN - Laboratori Nazionali di Frascati

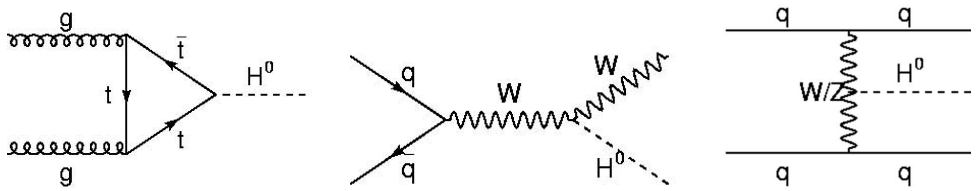

Fig. 1. – Higgs boson production mechanisms gluon fusion (left), associated production (center), and vector boson fusion (right).

summer 2008 combination is about $3.0\,\mathrm{fb}^{-1}$, although some channels may be higher or lower.

2. – Higgs boson phenomenology

At the Tevatron, there are three experimentally important mechanisms of Higgs boson production, which are gluon fusion, vector boson associated production, and vector boson fusion (fig. 1). The dominant decay modes of the Higgs boson are $H \to b\bar{b}$ for $m_H < 135\,\mathrm{GeV}$ and $H \to WW$ for $m_H > 135\,\mathrm{GeV}$. Other decay modes are much smaller than one of these decays at all Higgs masses, but may be experimentally significant nonetheless due to smaller backgrounds.

The combination of Higgs boson production and decay determines the complete experimental signature. Various signatures have been determined to be viable methods of searching for the Standard Model Higgs boson at the Tevatron. The two most important signatures are $VH \to \ell\ell' b\bar{b}$ for low Higgs boson masses ($m_H < 135\,\mathrm{GeV}$), and $H \to WW \to \ell\ell'\nu\nu'$ (opposite-sign dilepton) for high Higgs boson masses ($m_H > 135\,\mathrm{GeV}$). In this paper, we are concerned with the latter, plus two additional signatures $WH \to WWW \to \ell^{\pm}\ell^{\pm} + X$ (like-sign dilepton) and $H \to \gamma\gamma$.

3. – $H \to WW$

The most sensitive channel for Higgs boson searches is the high-mass region at the Tevatron is the opposite-sign dilepton channel $H \to WW \to \ell\ell$, with maximum sensitivity around $m_H = 160\,\mathrm{GeV}$. The experimental signature is two high-p_T, isolated, opposite-sign leptons ($\ell = e$ or μ) and missing transverse energy. There are three subchannels corresponding to $\ell\ell = ee$, $e\mu$, and $\mu\mu$. The major backgrounds are diboson (WW, WZ, ZZ), $Z \to \ell\ell$, $Z \to \tau\tau$, and fake lepton backgrounds from $W + \gamma$/jets and QCD multijets.

The WW diboson background is a fundamental physics background, and one of the largest backgrounds. The most sensitive variable for distinguishing Higgs boson signal from the WW diboson background is the dilepton azimuthal opening angle $\Delta\phi_{\ell\ell}$. In the case of Higgs boson signal, the two charged leptons tend to be emitted in the same direction (small $\Delta\phi_{\ell\ell}$) due to spin correlation, whereas in the case of diboson (and other) background, the two charged leptons tend to be emitted back-to-back ($\Delta\phi_{\ell\ell}$ close to π). The dilepton opening angle is not the only variable that is useful for distinguishing signal from background, however. Therefore, both experiments have used multivariate techniques, including neural networks (NN), boosted decision trees (BDT) and matrix element (ME) to get the best possible sensitivity.

TABLE I. – *Preselection cuts for $H \to WW$.*

		ee	$e\mu$	$\mu\mu$
CDF	Leptons	$p_{T1} > 20\,\text{GeV}$, $p_{T2} > 10\,\text{GeV}$, $m_{\ell\ell} > 16\,\text{GeV}$		
	$\not\!\!E_{T\text{spec}}$ (GeV)	> 25	> 15	> 25
D0	Leptons	$p_{T\mu} > 10\,\text{GeV}$, $p_{Te} > 15\,\text{GeV}$, $m_{\ell\ell} > 15\,\text{GeV}$		
	$\not\!\!E_T$ (GeV)	> 20	> 20	> 20
	$\not\!\!E_T^{\text{scaled}}$	> 7	> 6	> 5
	$M_T^{\min}$ (GeV)	> 20	> 30	> 20
	$\Delta\phi_{\ell\ell}$	< 2.0	< 2.0	< 2.5

3˙1. *CDF $H \to WW$ analysis.* – The CDF result for the $H \to WW$ channel has been updated since the summer 2008 Higgs combination with a new result based on an integrated luminosity of $3.6\,\text{fb}^{-1}$ [4]. The preselection cuts are shown in table I. The preselection makes use of a modified missing E_T variable called $\not\!\!E_{T\text{spec}}$, which is the ordinary $\not\!\!E_T$ multiplied by the sine of $\Delta\phi$ from the $\not\!\!E_T$ vector to the nearest charged lepton or jet (if $\Delta\phi < \pi/2$).

Additional analysis after the preselection stage is based on neural networks (NN). Separate NNs are used for 0, 1, and 2 or more jets. The 0-jet subsample uses a 5-variable NN. The 1- and 2-or-more-jet subsamples use an 8-variable NN. Additionally, the 0- and 1-jet subsamples are further subdivided high– and low–signal-to-background subsamples based on the quality of the lepton identification. This subdivision is motivated by the fact that different backgrounds are important in these cases. Distributions of the NN output are shown in figs. 2–4.

The Higgs boson cross-section times branching ratio is obtained from a simultaneous likelihood fit of all five NN distributions. The 95% CL upper limit on Higgs boson production relative to the SM prediciton is shown in fig. 5.

3˙2. *D0 $H \to WW$ analysis.* – The D0 result for the $H \to WW$ channel is based on an integrated luminosity of $3.0\,\text{fb}^{-1}$ [5]. The variables used for preselection include $\not\!\!E_T^{\text{scaled}}$, which is an approximation of the missing E_T significance, $M_T^{\min}$ which is the minimal transverse mass of either charged lepton and the missing E_T, and the charged lepton azimuthal opening angle $\Delta\phi_{\ell\ell}$ as described at the beginning of this section. Subsequent

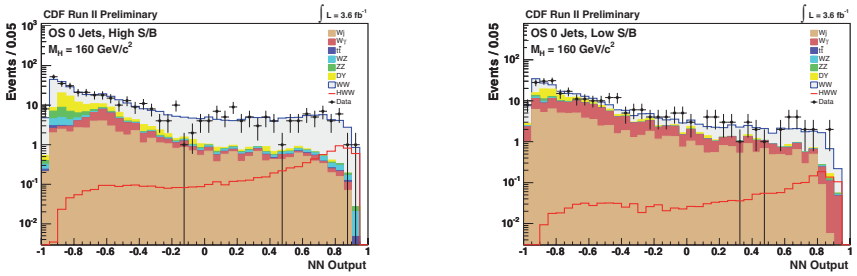

Fig. 2. – CDF $H \to WW + 0$ jets NN distributions for high-(S/B) (left) and low-(S/B) (right) lepton identification.

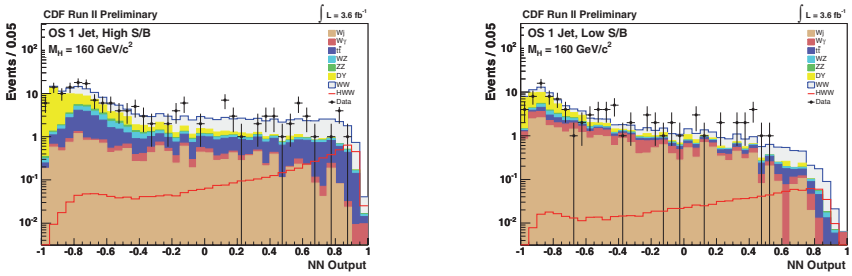

Fig. 3. – CDF $H \to WW + 1$ jets NN distributions for high-(S/B) (left) and low-(S/B) (right) lepton identification.

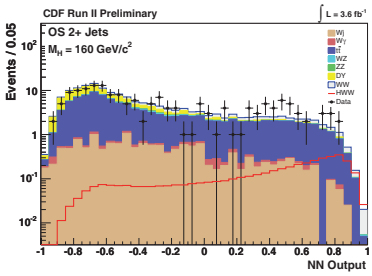

Fig. 4. – CDF $H \to WW + 2$ jets NN distributions.

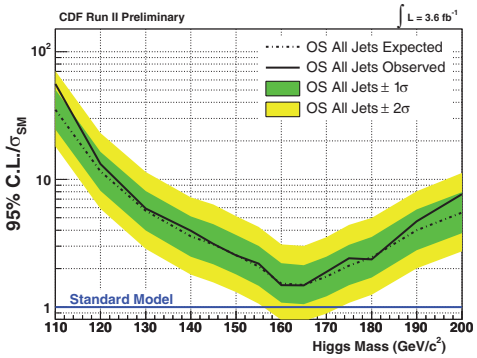

Fig. 5. – CDF $H \to WW$ upper limit on Higgs boson production relative to SM prediction.

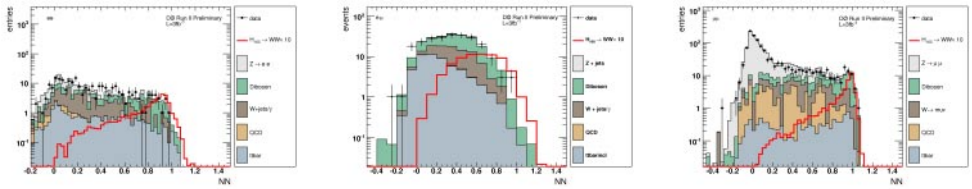

Fig. 6. – D0 $H \to WW$ NN distribution for ee (left), $e\mu$ (center), $\mu\mu$ (right).

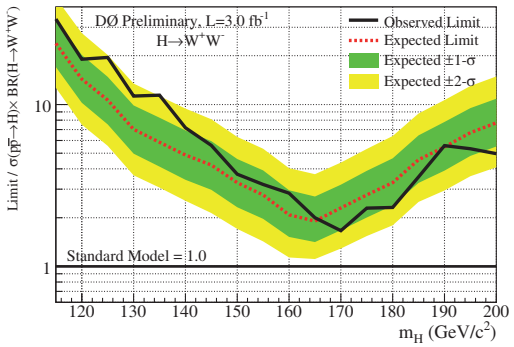

Fig. 7. – D0 $H \to WW$ upper limit on Higgs boson production relative to SM prediction.

analysis is based on a 14-variable neural network. The NN output for the three subchannels is shown in fig. 6. The observed NN distribution is consistent with background. The 95% CL upper limit on Higgs boson production relative to the SM predicion is shown in fig. 7.

4. – $WH \to WWW$

The second channel we are considering in this paper is $WH \to WWW \to \ell^{\pm}\ell^{\pm} + X$. The signature is two like-sign leptons ($\ell = e$ or μ). The cross-section time branching ratio is smaller than the $H \to WW$ channel, but the background is also lower. Physics background comes from diboson production (WZ and ZZ), but instrumental backgrounds (charge flips and fake leptons) are dominant.

4˙1. *CDF $WH \to WWW$.* – The CDF result for the $WH \to WWW$ channel has been updated since the summer 2008 Higgs combination with a new result based on an integrated luminosity of $3.6\,\text{fb}^{-1}$ [6]. Preselection cuts for this channel are two like-sign leptons (e or μ) with $p_T > 20\,\text{GeV}$. Subsequent analysis is based on a 13-variable neural network. The measured Higgs boson $\sigma \times BR$ is based on a likelihood fit of the NN distribution. No excess events above background are observed. The NN distribution and 95% CL upper limits on Higgs boson production are shown in fig. 8.

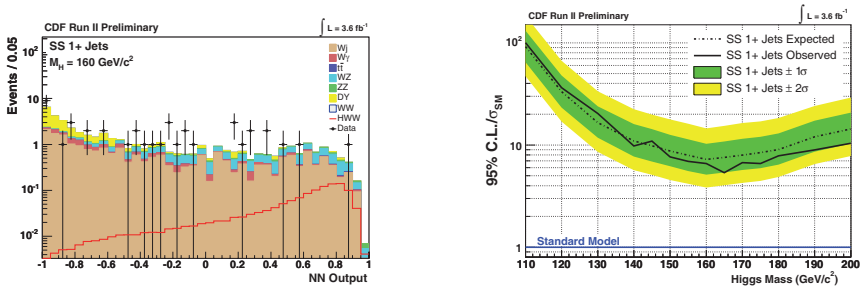

Fig. 8. – CDF $WH \to WWW$ NN distribution (left) and 95% CL upper limit on Higgs boson production relative to SM prediction (right).

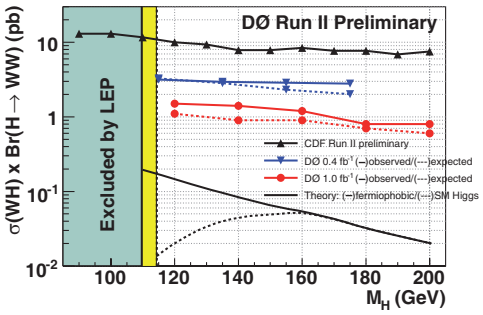

Fig. 9. – D0 $WH \to WWW$ 95% CL upper limit on Higgs boson production.

4˙2. *D0 $WH \to WWW$.* – The D0 result for the $WH \to WWW$ channel is based on an integrated luminosity of $1.1\,\mathrm{fb}^{-1}$ [7]. Preselection cuts are two like-sign leptons (e or μ) with $p_T > 15\,\mathrm{GeV}$. Higgs production is measured using a 2-dimensional multivariate likelihood fit. No excess above background is observed. The 95% CL upper limit on Higgs production is shown in fig. 9.

4˙3. *Tevatron high-mass Higgs combined limit.* – The results shown in this section are from the summer 2008 Tevatron high-mass Higgs combination [3], which includes results from the $H \to WW$ (opposite-sign dilepton) and $WH \to WWW$ (like-sign dilepton) channels from both experiments, taking into account correlated systematic errors. The result of this combination is often displayed as a log-likelihood ratio (LLR), defined as

$$LLR(m_H) = -2\ln\frac{P(\mathrm{data}|m_H)}{P(\mathrm{data}|\mathrm{Null})}\,, \tag{1}$$

where $P(\mathrm{data}|\mathrm{hypothesis})$ is the probability of obtaining a particular experimental outcome ("data") assuming a given hypothesis. Figure 10 shows $LLR(m_H)$ and the 95% CL upper limit on Higgs boson production relative to the SM prediction. By way of interpretation, the maximum expected sensitivity occurs when the LLR corresponding to the null hypothesis (black dashed line) has the maximum separation from the LLR corresponding to the Higgs mass hypothesis (red dashed-dotted line). The maximum

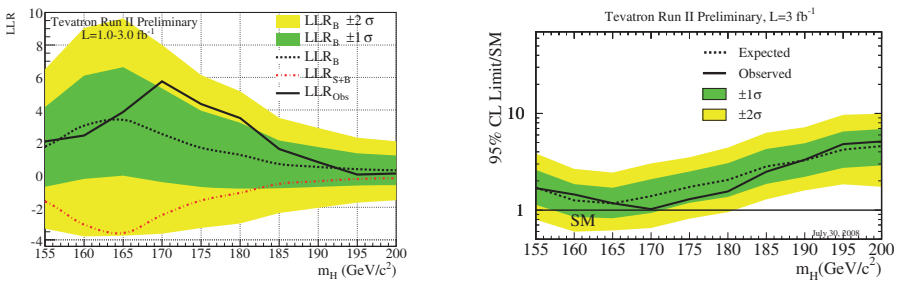

Fig. 10. – (Colour on-line) $LLR(m_H)$ (left) and 95% CL upper limit on Higgs production relative to SM prediction (right).

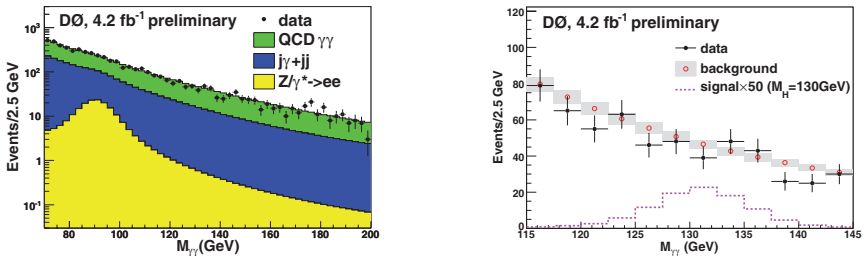

Fig. 11. – D0 $H \to \gamma\gamma$ diphoton invariant-mass distributions.

actual sensitivity occurs when the LLR corresponding to the observed data (black solid line) has the maximum separation from the LLR corresponding to the Higgs mass hypothesis (red dashed-dotted line). The latter occurs at $m_H = 170\,\text{GeV}$, and in fact m_H is excluded at 95% CL. The LLR is calculated at 5 GeV intervals, and m_H is the only excluded point.

5. – $H \to \gamma\gamma$

The Higgs boson decay $H \to \gamma\gamma$ has a fairly small branching ration (maximum about 0.2%), but it is still interesting for several reasons. The branching ratio for $H \to \gamma\gamma$ is maximum in the intermediate mass range $m_H \sim 120$–$130\,\text{GeV}$, where the sensitivity of the dilepton and associated production modes is weakest. Additionally, the $H \to \gamma\gamma$ channel can have enhanced importance in several non-SM scenarios, including the four-generation and fermiphobic Higgs scenarios (although the limites presented here only directly apply to the SM case).

The signature for the $H \to \gamma\gamma$ channel is two high-p_T isolated photons forming a narrow invariant mass peak at the Higgs boson mass. An important and fundamental physics background is nonresonant QCD $\gamma\gamma$ production. There are also instrumental backgrounds jets faking photons (QCD γ + jet and dijet) and electrons faking photons (Z and Drell-Yan ee production).

5˙1. *D0 $H \to \gamma\gamma$.* – D0 has a new SM $H \to \gamma\gamma$ result based on an integrated luminosity of $4.2\,\text{fb}^{-1}$ [8]. Event selection requires two photons with tight photon identification,

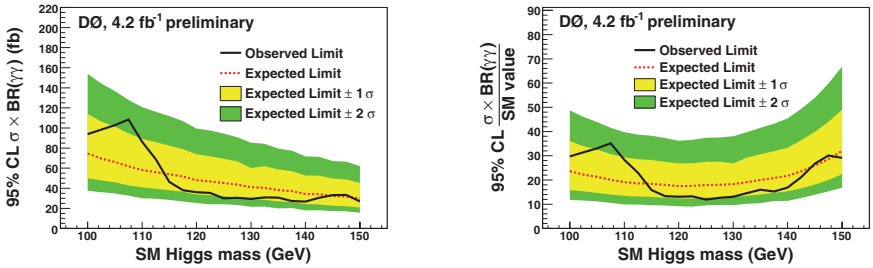

Fig. 12. – D0 $H \to \gamma\gamma$ 95% CL upper limit on Higgs boson production shown as absolute $\sigma \times BR$ (left) and relative to SM prediction (right).

with $E_T > 25\,\text{GeV}$ and pseudorapidity $|\eta| < 1.1$. The invariant mass spectrum of $\gamma\gamma$ events is shown in fig. 11 for the different background contributions (left) and comparing background and the expected signal for a particular Higgs boson mass (right). The observed events are consistent with the expected background. The Higgs boson $\sigma \times BR$ is measured as a function of m_H using the expected Higgs boson lineshape (fig. 11 right). The 95% CL upper limit on Higgs boson production is shown in fig. 12.

6. – Conclusions

Results have been presented from the CDF and D0 experiments for the Higgs boson channels $H \to WW$, $WH \to WWW$ and $H \to \gamma\gamma$. Combined results from the first two channels (the Tevatron summer 2008 high-mass Higgs combination) have been presented which exclude SM Higgs boson production at $m_H = 170\,\text{GeV}$.

* * *

We thank the staffs at Fermilab and collaborating institutions, and acknowledge support from the DOE and NSF (USA); CEA and CNRS/IN2P3 (France); FASI, Rosatom and RFBR (Russia); CNPq, FAPERJ, FAPESP and FUNDUNESP (Brazil); DAE and DST (India); Colciencias (Colombia); CONACyT (Mexico); KRF and KOSEF (Korea); CONICET and UBACyT (Argentina); FOM (The Netherlands); STFC and the Royal Society (United Kingdom); MSMT and GACR (Czech Republic); CRC Program, CFI, NSERC and WestGrid Project (Canada); BMBF and DFG (Germany); SFI (Ireland); The Swedish Research Council (Sweden); CAS and CNSF (China); and the Alexander von Humboldt Foundation (Germany).

REFERENCES

[1] Barate R. *et al.*, *Phys. Lett. B*, **565** (2003) 61.
[2] LEP Electroweak Working Group, arXiv:0712.0929 [hep-ex] and `http://lepewwg.web.cern.ch/LEPEWWG/`.
[3] Tevatron New Phenomena & Higgs Working Group, arXiv:0808.0534v1 [hep-ex] and `http://tevnphwg.fnal.gov/`.
[4] CDF Collaboration, CDF Note 9764.
[5] D0 Collaboration, D0 Note 5757-CONF.
[6] CDF Collaboration, CDF Note 9764.
[7] D0 Collaboration, D0 Note 5485-CONF.
[8] D0 Collaboration, D0 Note 5858-CONF.